

The Smoking Guns Of Short Hard Gamma Ray Bursts

Shlomo Dado and Arnon Dar
Physics Department, Technion, Haifa, Israel

The X-ray afterglow of short hard bursts (SHBs) of gamma rays provides compelling evidence that SHBs are produced by highly relativistic jets launched in the birth of rotationally powered millisecond pulsars (MSPs) in merger of neutron stars and/or in mass accretion on neutron stars in low mass X-ray binaries. Gravitational wave detection of relatively nearby neutron star mergers by Ligo-Virgo, followed by far off-axis short GRBs or orphan afterglows of beamed away SHBs with an MSP-like light curve will verify beyond doubt the neutron star merger origin of SHBs.

PACS numbers: 98.70.Sa,97.60.Gb,98.20

I. INTRODUCTION

Gamma ray bursts seem to be divided into two distinct classes, long duration soft gamma ray bursts (GRBs) that usually last more than 2 seconds and short hard bursts (SHBs) that usually last less than 2 seconds [1]. While there is clear observational evidence for production of long duration GRBs in broad line supernova explosions of type Ic [2], the origin of SHBs (and of SN-less GRBs) is still unknown. Supernova origin is ruled out [3], and although there is no solid evidence, it is widely believed [4] that SHBs are produced mainly in merger of neutron stars in close binaries [5]. SHBs are often followed by extended emission (EE) with a much lower luminosity that lasts a couple of minutes and is taken over during its fast decay phase by a long duration afterglow [6]. The origin of the EE and the afterglow of SHBs are also not known [4], although it has been suggested long ago that rotationally powered millisecond pulsars (MSPs) or magnetars powered by magnetic energy, which are born in neutron star mergers, dominate or contribute to the afterglow of SHBs [7]. Recently, this possibility has attracted increasing attention [8], but all past attempts to model the X-ray afterglow of SHBs with jet plus magnetar emission were based on rather heuristic functions with free adjustable parameters rather than on formulae derived from the underlying model.

In this letter, we show that the X-ray light curves of the afterglow of SHBs, which were measured with the Swift X-ray telescope (XRT) are indeed those expected from the launch of highly relativistic narrowly collimated jets which produce the SHBs in the birth of rotationally powered MSPs. Such MSPs are the smoking guns from the production of SHBs. They seem to be present in all SHBs, which rules out the birth of stellar black holes or magnetars powered by the decay of ultra-strong magnetic field as the origin of most SHBs. The highly relativistic jets that produce SHBs in neutron star mergers [5,9] or/and in phase transition of neutron stars to more compact stars (quark stars ?) in compact binaries, within or without globular clusters [10], produce the SHBs with or without an EE, respectively. In SHBs with an EE that are produced within dense stellar regions, such as the collapsed cores of globular clusters, the MSP powered X-ray

emission takes over only during the fast decay phase of the EE.

II. JETTED SHBS

If SHBs, like GRBs, are produced by highly relativistic narrowly collimated bipolar jets of plasmoids with a large bulk motion Lorentz factor $\gamma \gg 1$, through inverse Compton scattering (ICS) of external light, then they are expected to have many similar properties [9,10,11]: Both are narrowly beamed, mostly viewed from an angle $\theta \approx 1/\gamma$ relative to the jet direction of motion, and consequently, both are expected to display a large linear polarization, $\Pi = 2\gamma^2 \theta^2 / (1 + \gamma^4 \theta^4) \approx 1$ [9,11]. The peak energy of their time integrated energy spectrum satisfies $(1+z)Ep \propto \gamma\delta$, while their isotropic equivalent total gamma ray energy satisfies $E_{iso} \propto \gamma\delta^3$, where z is their redshift and $\delta = 1/\gamma(1 - \beta \cos\theta)$ is their Doppler factor. Hence, ordinary GRBs and SHBs, that are mostly viewed from an angle $\theta \approx 1/\gamma$, were predicted to satisfy the correlation $(1+z)Ep \propto [E_{iso}]^{1/2}$, while far off-axis ($\theta^2 \gg 1/\gamma^2$) GRBs and SHBs were predicted to satisfy $(1+z)Ep \propto [E_{iso}]^{1/3}$ [12]. All these predictions are well satisfied by GRBs, but so far, because of observational limitations, only the correlation $(1+z)Ep \propto [E_{iso}]^{1/2}$ for near axis (ordinary) SHBs could be verified, as shown in Figure 1.

III. AFTERGLOW POWERED BY MSPS

Young X-ray pulsars seem to be surrounded by nearby plerions, which absorb their emitted radiation, winds, and highly relativistic particles, and convert them to luminous energy, mostly in the X-ray band. Observations indicate that the change of their period P during their spin down satisfies to a good approximation,

$$P\dot{P} = K \quad (1)$$

where K is time independent constant. Such a behavior is expected from pulsars which spin down in vacuum by magnetic dipole radiation (MDR) [13]. But $P\dot{P}$ seems to remain constant to a good approximation also when

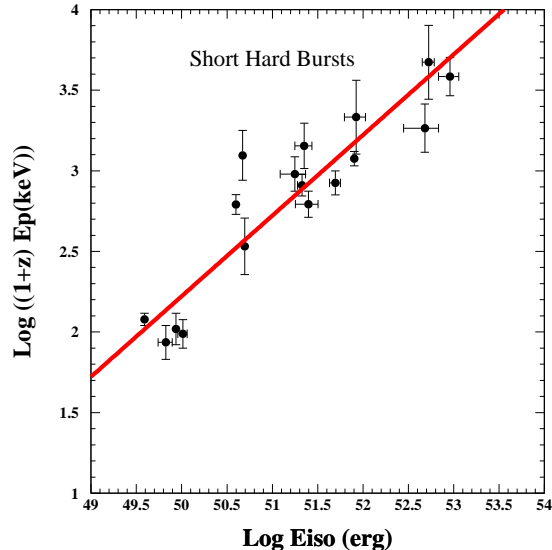


FIG. 1: The measured rest frame peak energy $(1+z)Ep$ as function of the equivalent isotropic gamma-ray energy E_{iso} of SHBs with known redshift z . The line is the expected correlation $(1+z)Ep \propto E_{iso}^{1/2}$ for ordinary (near axis) SHBs produced by ICS of light by highly relativistic jets. Far off-axis short GRBs are expected to satisfy $(1+z)Ep \propto E_{iso}^{1/3}$.

other spin down mechanisms, such as emission of winds and/or highly relativistic particles, contribute, or even dominate the spin-down of pulsars. This is suggested by the fact that the age estimate $t = [P^2(t) - P^2(0)]/2K$ and the braking relation $d^2P/dt^2 \approx -K^2/P^3$ [13] seem to be well satisfied by young X-ray pulsars: The ages obtained from the age relation are consistent with the known ages of their parent supernovae (historical supernova) and/or their ages obtained from measurements of the distance and proper motion of the young pulsars relative to the centers of the supernova remnants where they were born. The braking relation, which is very difficult to test over a human time scale, has been verified only in few young X-ray pulsars where it yielded a braking index near the expected value 3 [14].

Eq.(1) yields a time-dependent period

$$P(t) = P_i(1 + t/t_b)^{1/2}, \quad (2)$$

where $P_i = P(0)$ is the initial period of the neutron star, t is the time after its birth, and $t_b = P_i/2\dot{P}_i$.

If the rotational energy loss of a neutron star with a constant moment of inertia I powers its luminosity L and if $P\dot{P}$ remains constant as function of time, then its luminosity $L = I\omega\dot{\omega}$ where $\omega = 2\pi/P$ satisfies

$$L_{ps}(t) = L_{ps}(0)(1 + t/t_b)^{-2}. \quad (3)$$

The afterglow of a GRB at redshift z that is powered by such a luminosity has a local energy flux density $F(t) =$

$L(t)/4\pi D_L^2$, where D_L is the luminosity distance of the GRB at redshift z , i.e.,

$$F_{ps}(t) = F_{ps}(0)(1 + t/t_b)^{-2}. \quad (4)$$

If only a fraction η of the rotational energy loss is converted to X-rays, then

$$P_i = \frac{1}{D_L} \sqrt{\frac{(1+z)\pi\eta_x I}{2F_{ps,x}(0)t_b}}, \quad (5)$$

For a canonical neutron star of a radius $R = 10^6$ cm and a mass $M \approx M_{Ch}$, where $M_{Ch} \approx 1.4M_\odot$ is the Chandrasekhar mass limit of white dwarfs, the moment of inertia has the value $I = (2/5)M_{Ch}R^2 \approx 1.12 \times 10^{45} g cm^2$.

IV. LIGHT CURVES POWERED BY MAGNETARS

The standard estimate [13] of the magnetic field of pulsars is valid only for MSPs in vacuum, which spin down by emitting magnetic dipole radiation (MDR). It overestimate the magnetic field if other power sources dominate their electromagnetic radiation and is unreliable for distinguishing between highly magnetized MSPs and magnetars. Therefore we shall adhere to the original definition of magnetars, namely pulsars whose luminosity is powered by their ultra strong magnetic field energy, rather than by their rotational energy or other intrinsic power sources.

A magnetic dipole \mathbf{m} of a neutron star of a radius R produces a magnetic field whose peak surface value $B = 2m/R^3$ is at its magnetic poles, and its total magnetic field energy is $U \approx B^2 R^3/12$. If the magnetic dipole is aligned at an angle α relative to the rotation axis of the neutron star whose spin period is P , then it emits MDR at a rate [15],

$$L = \frac{8\pi^4 B^2 R^6 \sin^2\alpha}{3c^3 P^4}. \quad (6)$$

However, since both L and U are proportional to B^2 , the observed luminosity of such magnetars decreases like

$$L(t) = L(0)(P_i/P)^4 \exp(-\int dt/\tau) \quad (7)$$

where $\tau = c^3 P^4/64\pi^4 R^3 \sin^2\alpha$. As long as $P(t) \approx P_i$,

$$L(t) = L(0) \exp(-t/\tau). \quad (8)$$

The different light-curves of MSPs powered by rotation energy and of magnetars powered by magnetic field energy, as given, respectively, by Eq.(4) and Eq.(8), can tell which one of these sources, if any, can reproduce the light-curves of the X-ray afterglows of SHBs and be identified as the smoking gun of SHBs.

Figures 2,3 show the well sampled X-ray afterglow of two representative SHBs without EE, 130603B and

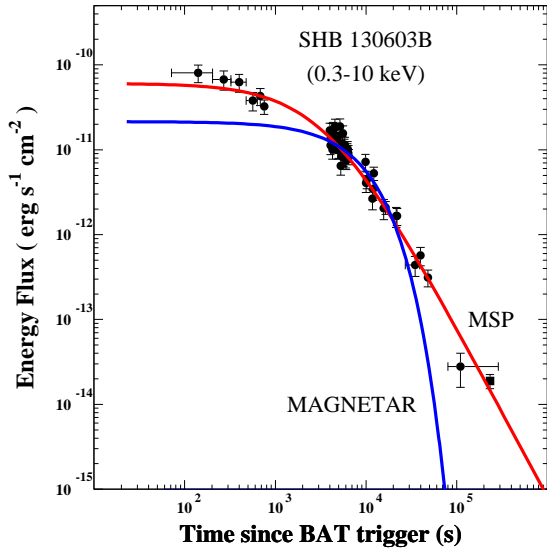


FIG. 2: The light curve of the X-ray afterglow of SHB 130603B reported in the Swift-XRT GRB light curve repository [16] and its best fit light curves of MSP powered by rotation or by a magnetar powered by magnetic field energy, as given by Eqs. (4) and (8), respectively, with the parameters listed in table I.

090510, which were reported in the Swift-XRT GRB light curve repository [16] and their best fit MSP and magnetar powered light curves as given, respectively, by Eq.(4) and Eq.(8). As demonstrated in figures 2,3, while Eq.(4) for rotationally powered MSPs fit well the X-ray afterglows of SHBs 130603B and 090510 without EE [16], the magnetar light curves, which are powered by magnetic field energy, as given by Eq.(8), do not. This is valid for all the well sampled X-ray afterglows of SHBs without EE that are reported in the Swift-XRT GRB light curve repository [16].

V. SHBS WITH AN EXTENDED EMISSION.

A considerable fraction of SHBs may take place in rich star clusters, such as globular clusters (GCs) [10], in particular within collapsed cores (CCs) of GCs where the ratio of binary neutron stars and MSPs to ordinary stars is much higher than in the regular interstellar medium of galaxies. ICS of the ambient light around the birth place of the MSP within the GCs by the highly relativistic jet/plasmoid, which produces the SHB, can also produce the extended emission (EE). Inside the GC where the light is nearly isotropic, the EE is proportional to the light density along the plasmoid's trajectory. Far outside the GC, the intercepted light has a small angle relative to the plasmoid direction of motion. At a distance r from a GC of a radius R , the energy ϵ_γ of the intercepted photons is Lorentz transformed to $\approx (R/r)\epsilon_\gamma$

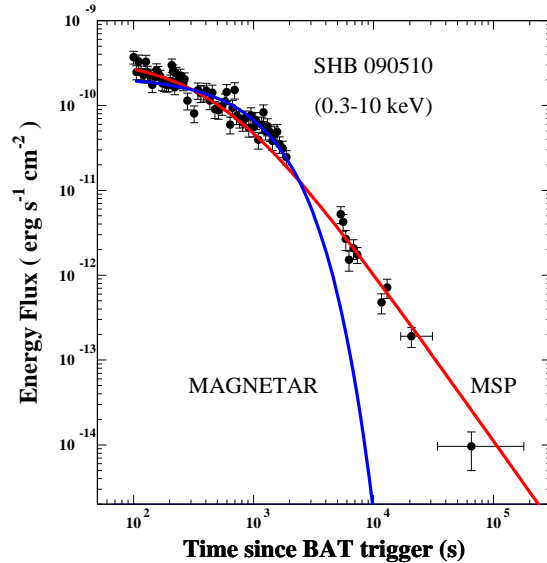


FIG. 3: The light curve of the X-ray afterglow of SHB 090510 reported in the Swift-XRT GRB light curve repository [16] and its best fit light curves of MSP powered by rotation or by a magnetar powered by magnetic field energy, as given by Eqs. (4) and (8), respectively, with the parameters listed in table I.

in the jet/plasmoid rest frame. This energy is boosted by ICS to an energy $E \approx \gamma \epsilon_\gamma R/(1+z)r$ when observed at a viewing angle $\theta \approx 1/\gamma$ in the rest frame of the distant observer. At observer time t , $r = \gamma \delta ct/(1+z)$. Hence, for a GC light with bremsstrahlung-like spectrum $\epsilon^2 dn/d\epsilon \propto \exp(-\epsilon/\epsilon_c)$ and a photon density $n_\gamma \propto 1/r^2$, the observed energy flux density of the EE due to ICS of GC light decays like

$$F_{ee}(t) \propto t^{-1} \exp(-t/t_{ee}) \quad (9)$$

with $t_{ee}(E) \approx 100 (R/pc)(\epsilon_c/eV)/c(E/keV)(\gamma/10^3)s$, which depends strongly on the observed energy band, and produces a fast spectral softening of the EE during its rapid decay phase. A succession of plasmoids or a non homogenous light density within the star cluster yield a bumpy EE light curve, which can be resolved because of the relatively large photon statistics. Later, when the luminosity decreases, the larger time bins (and perhaps merger of plasmoids) yield a smoothly appearing light curves. Hence, the smoothed X-ray light-curves of SHBs with EE, which are taken over by MSP, are expected to be described roughly by

$$F(t) \approx \frac{F_{ee} a_{ee}}{a_{ee} + (t/t_{ee}) \exp(t/t_{ee})} + \frac{F_p}{(1+t/t_b)^2}, \quad (10)$$

while those taken over by magnetars are expected to be described roughly by Eq.(10) with $1/(1+t/t_b)^2$ replaced by $\exp(-t/\tau)$. In Eq. (10), the parameter a_{ee} was introduced for the interpolation between a smoothed early

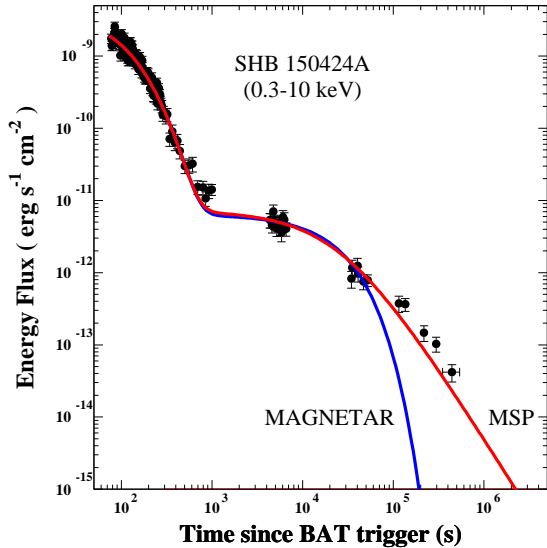


FIG. 4: The light curve of the X-ray afterglow of SHB 150424A reported in the Swift-XRT GRB light curve repository [16] and its best fit light curves of MSP powered by rotation or by a magnetar powered by magnetic field energy, as given by Eqs. (4) and (8), respectively, with the parameters listed in table I.

time EE behavior and its late time analytic description (Eq. (9)).

VI. COMPARISON WITH OBSERVATIONS

Figures 4,5 show the X-ray afterglow of two representative SHBs with EE, 150424A and 060313, with well sampled light curves reported in the Swift-XRT GRB light curve repository [16]. Also shown are their best fit light curves obtained from Eq.(10) with essentially 4 adjustable parameters (2 for the decline of EE and 2 for the MSP or magnetar contribution). As shown in figures 2-5 and in figures 6-9 in the appendix, Eq.(10) fits well the X-ray lightcurves of all the 20 well sampled X-ray afterglows of bursts with a secured SHB identity, which are reported todate in the Swift-XRT GRB light curve repository [16]. The best fit parameters are listed in Table I.

Conclusions: All the well sampled X-ray afterglow of SHBs [16] provide compelling evidence that most SHBs are produced by highly relativistic jets which are launched in the birth of rotationally powered MSPs, and not in the birth of stellar black holes or magnetars powered by magnetic field energy:

The observed $E_p - E_{iso}$ correlation shown in Figure 1 for near axis SHBs is that expected from ICS of light by highly relativistic jets. The correlation $(1+z)E_p \propto E_{iso}^{1/3}$ for far off-axis SHBs could not be verified because of a small sample of such nearby SHBs. The ob-

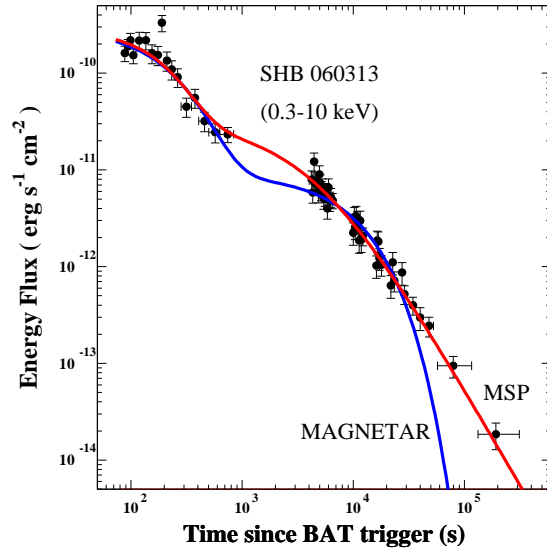


FIG. 5: The light curve of the X-ray afterglow of SHB 060313 reported in the Swift-XRT GRB light curve repository [16] and its best fit light curves of MSP powered by rotation or by a magnetar powered by magnetic field energy, as given by Eqs. (4) and (8), respectively, with the parameters listed in table I.

served fast decline phase of the EE with a rapid spectral softening [16] is well predicted by Eq.(9). The observed durations t_{ee} of the extended emission of SHBs are compatible with the typical size of the collapsed cores of rich globular clusters, which are the most likely sites of neutron star mergers. Measurements of the polarization of the prompt γ -rays and the EE of bright SHBs, with space based polarimeters such as Astrosat [17] and/or Polar [18] may provide a critical test of jet production mechanism of SHBs, which predicts a linear polarization, $\Pi \sim 1$ for near axis SHBs and their EE that declines to $\Pi \sim 0$ during the EE rapid decline phase.

MSP powered light curves fit very well the observed late-time X-ray afterglow of SHBs. The MSP periods P_i obtained from Eq.(6) are all well above the classical lower bound $2\pi R/c > 0.2 \text{ ms}$ for canonical neutron stars with a radius $R \approx 10^6 \text{ cm}$ (or of quark stars with smaller radii). The small periods are expected from the birth of MSPs in neutron star mergers or in the collapse of neutron stars to quark stars due to mass accretion in compact binaries [10].

The jet contribution to the observed prompt emission and EE phases overshines the MSP contribution during these phases. Absorption and re-emission of the MSP spin down energy by plerions probably turn a direct detection of a periodic MSP signal during the prompt and extended emission phases [19] to almost an impossible mission. However, the quasi-isotropic emission powered by the MSP is expected to be the only visible emission from far-off axis SHBs. Such emission from nearby MSPs

may be detected for days, months, and perhaps even years after their birth, and may explain the origin of some ultraluminous X-ray (ULX) sources [20]. The much smaller detection horizon of such orphan afterglows compared to that of near-axis SHBs, is over compensated by not being beamed. Gravitational wave detection of rela-

tively nearby ($D_L < 100$ Mpc) neutron star mergers by Ligo-Virgo, followed by the detection of far off-axis SHBs or an orphan afterglow of a beamed away SHB with an MSP-like light curve will verify the neutron star merger origin of SHBs.

-
- [1] J. P. Norris et al., *Nature*, **308**, 434 (1984); C. Kouveliotou et al., *ApJ*, **413**, L101 (1993), [arXiv:astro-ph/9809140].
- [2] For the first discovery see T. J. Galama et al., *Nature* **395**, 670 (1998), [arXiv:astro-ph/9806175]. For a recent review see, e.g., Z. Cano et al., *AdAst*, **2017**, 5 (2017), [arXiv:1604.03549], and references therein.
- [3] See, e.g., J. Hjorth et al., *Apj* **630**, L117 (2005), [arXiv:astro-ph/0506123]; E. Troja et al., *GCN Circular* 20222 (2016).
- [4] See, e.g., W. Fong, and E. Berger, *ApJ*, **776**, 18 (2013). For recent reviews see, e.g., E. Berger, *ARA&A*, **52**, 43, (2017 and references therein).
- [5] J. Goodman, A. Dar, and A. Nussinov, *ApJ*, **314**, L7 (1987), first suggested that gamma ray bursts may be produced in neutron star mergers by neutrino-antineutrino annihilation fireballs. Later, N. Shaviv and A. Dar, *ApJ*, **447**, 863 (1995) [arXiv:astro-ph/9407039] proposed that highly relativistic jets, rather than fireballs, emitted in neutron star mergers may produce gamma ray bursts by inverse Compton scattering.
- [6] The extended emission phase in SHBs following the prompt emission was first noticed by J. S. Villasenor et al., *Nature*, **437**, 855 (2005) and by J. P. Norris and J. T. Bonnell, *ApJ* **643**, 266 (2006), [arXiv:astro-ph/0601190].
- [7] Z. G. Dai and T. Lu, *PRL*, **81**, 4301 (1998), [arXiv:astro-ph/9810332]; Z. G. Dai and T. Lu, *A&A*, **333**, L87 (1988), [arXiv:astro-ph/9810402]; B. Zhang and P. Meszaros, *ApJ*, **552**, L35 (2001), [arXiv:astro-ph/0011133]; Z. G. Dai et al., *Science* **311**, 1127 (2006), [arXiv:astro-ph/0602525]; B. D. Metzger et al., *MNRAS*, **385**, 1455 (2008), [arXiv:0712.1233].
- [8] See, e.g., A. Rowlinson, A. Patruno, and P. T. O'Brien, arXiv:1706.08538; S. L. Gibson, et al. arXiv:1706.04802, F. Knust et al., arXiv:1707.01329, H. J. Lu et al. *ApJ*, **805** (2015), [arXiv:1501.02589], and references therein. Anomalous X-ray pulsars (AXPs) and soft gamma ray repeaters (SGRs) whose observed luminosity was found to exceed the loss-rate of their rotational energy [see, e.g., S. Mereghetti, *AAR*, **15**, 225 (2008), [arXiv:0804.0250], were the first pulsars which were claimed to be magnetars powered by the decay of their ultrastrong magnetic field.
- [9] N. Shaviv and A. Dar, *ApJ*, **447**, 863 (1995) [arXiv:astro-ph/9407039] and references therein.
- [10] S. Dado, A. Dar, and A. De Rújula, *ApJ*, **693**, 311 (2009), [arXiv:0807.1962].
- [11] A. Dar and A. De Rújula, *PhR*, **405**, 203 (2004), [arXiv:astro-ph/0308248].
- [12] A. Dar and A. De Rújula, [arXiv:astro-ph/0012227].
- [13] R. N. Manchester and J. H. Taylor, 1977, *Pulsars* (W. H. Freeman and Company, San Francisco 1977)
- [14] R. F. Archibald, E. V. Gotthelf, R. D. Ferdman, et al. *ApJ*...**819**, L16 (2016), [arXiv:1603.00305]
- [15] J. D. Jackson, *Classical Electrodynamics* (Wiley, New York, 1999), 3rd ed.
- [16] P. A. Evans et al., *MNRAS*, **397**, 1177 (2009), [arXiv:0812.3662]; P. A. Evans et al., *A&A*, **469**, 379 (2007), [arXiv:0704.0128].
- [17] T. Chattopadhyay et al., arXiv:1707.06595, and references therein.
- [18] M. Kole et al., arXiv:1708.00664, and references therein.
- [19] A. Rowlinson, A. Patruno, and P. T. O'Brien, arXiv:1706.08538.
- [20] K. Makishima et al., *ApJ*, **535**, 632 (2000), [arXiv:astro-ph/0001009]; A. R. King et al., *ApJ*, **552**, L109 (2001), [arXiv:astro-ph/0104333].

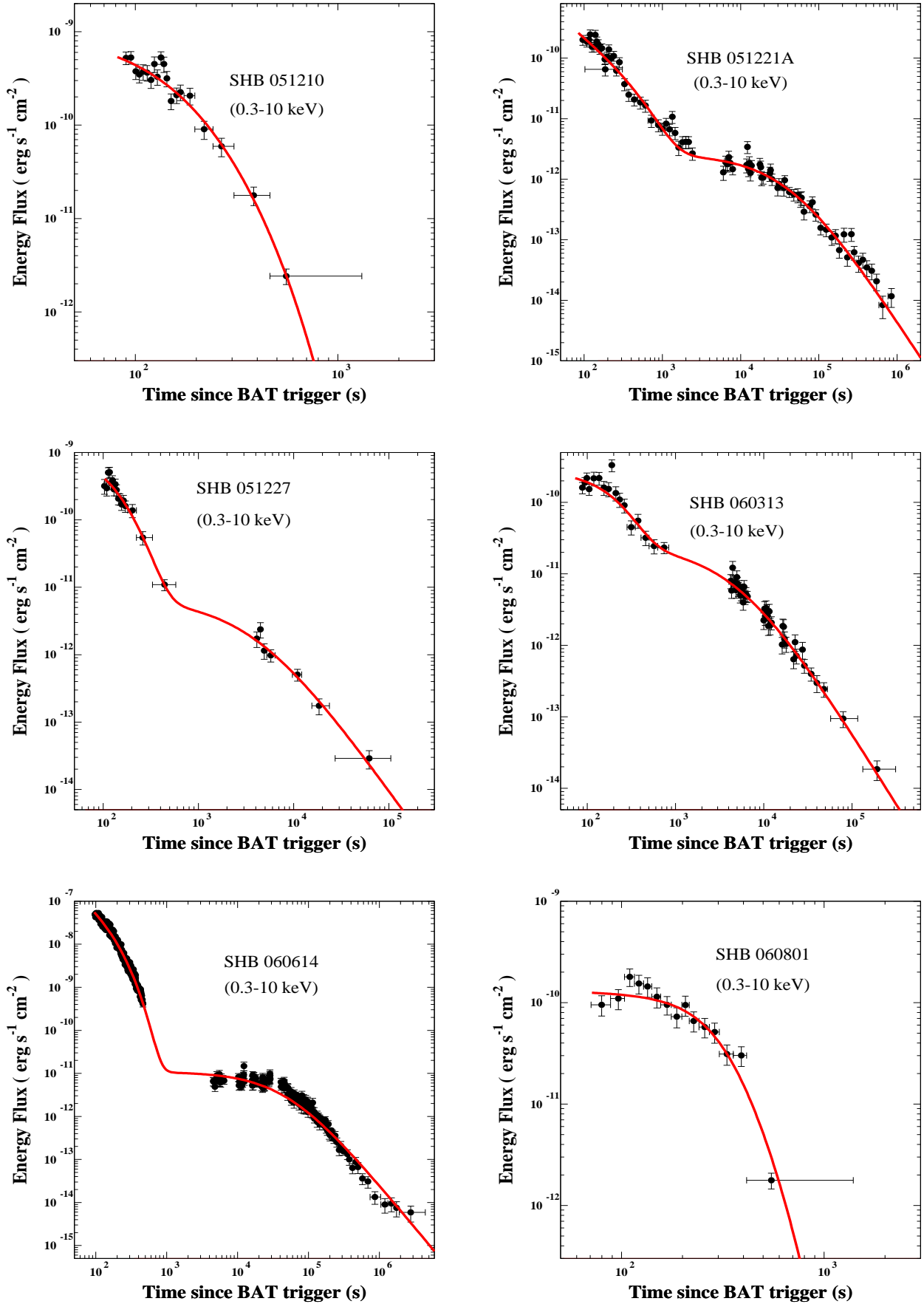


FIG. 6: The X-ray light curve of SHBs 051210, 051221A, 051227, 060313, 060614, and 060801 reported in the Swift-XRT GRB light curve repository [16] and their best fit light curves assuming ICS of GC light by a highly relativistic jet taken over by MSP afterglow, as given by Eq.(4) or Eq.(10) with the 2 or 4 parameters, respectively, listed in Table I.

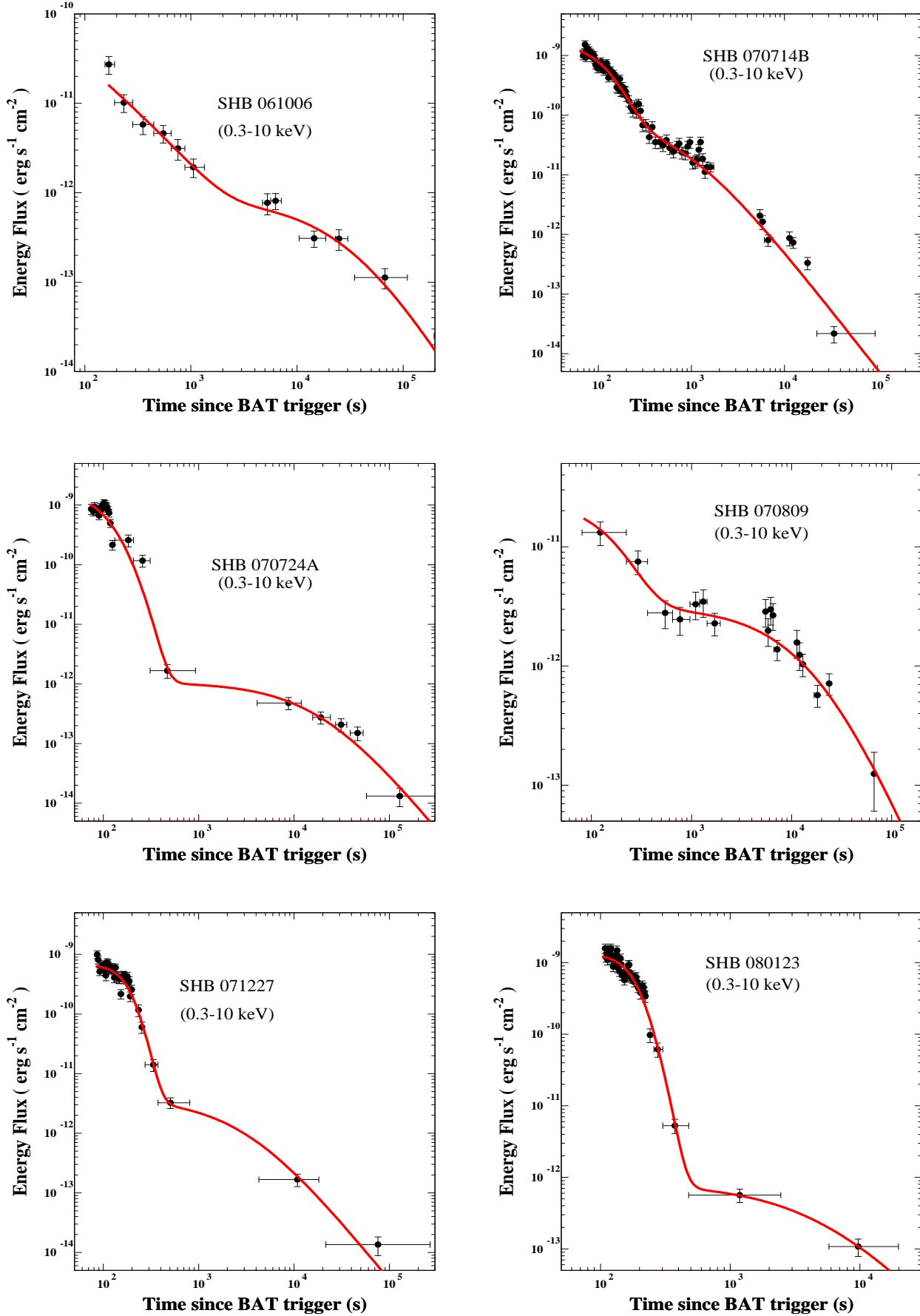


FIG. 7: The X-ray light curve of SHBs 061006, 070714B, 070724A, 070809, 071227, and 080123 reported in the Swift-XRT GRB light curve repository [16] and their best fit light curves assuming ICS of GC light by a highly relativistic jet taken over by MSP afterglow, as given by Eq.(4) or Eq.(10) with the 2 or 4 parameters, respectively, listed in Table I.

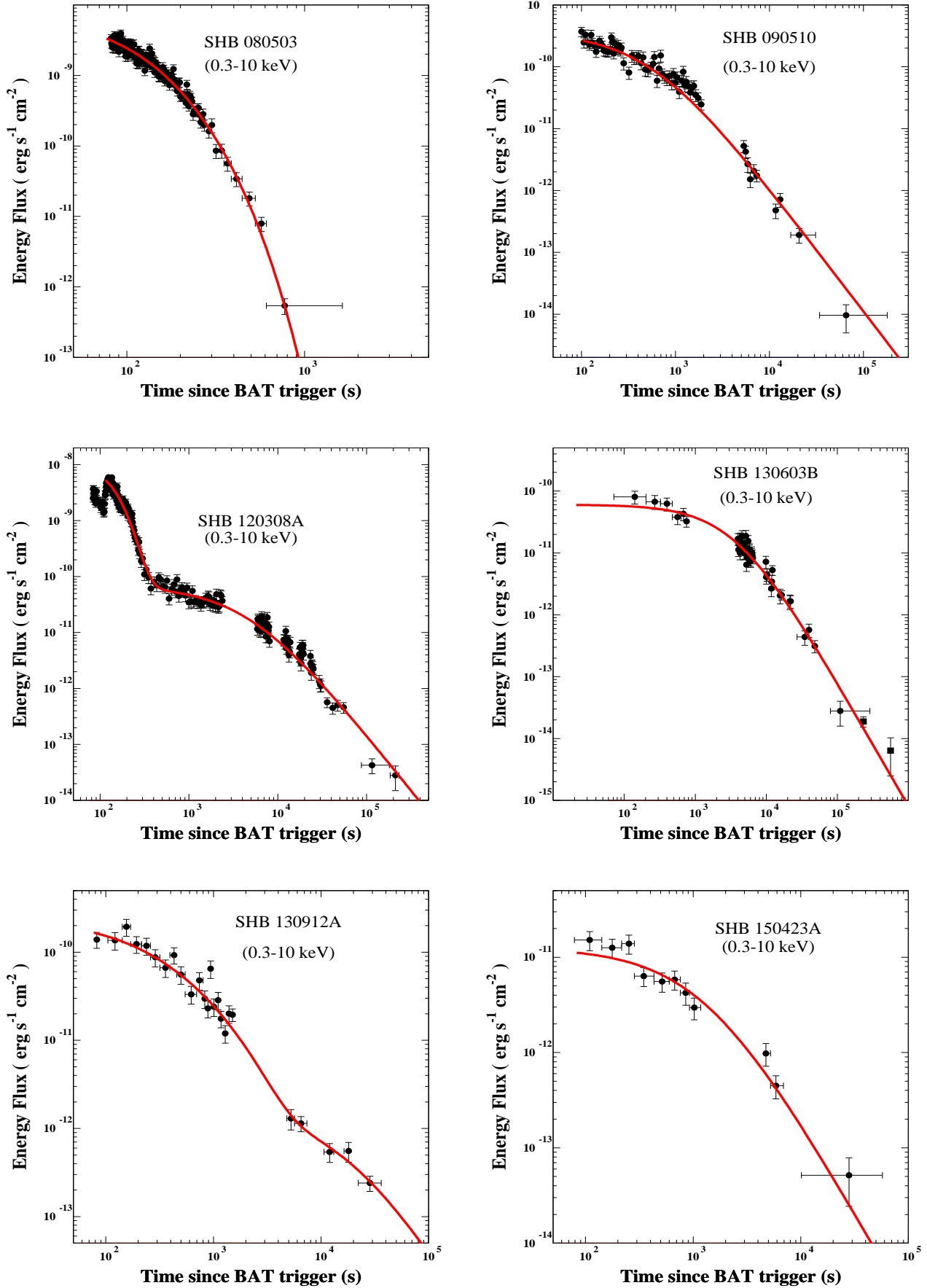


FIG. 8: The X-ray light curve of SHBs 080503, 090510, 120308A, 130603, 130912A, 150423A reported in the Swift-XRT GRB light curve repository [16] and their best fit light curves assuming ICS of GC light by a highly relativistic jet taken over by MSP afterglow, as given by Eq.(4) or Eq.(10) with the 2 or 4 parameters, respectively, listed in Table I.

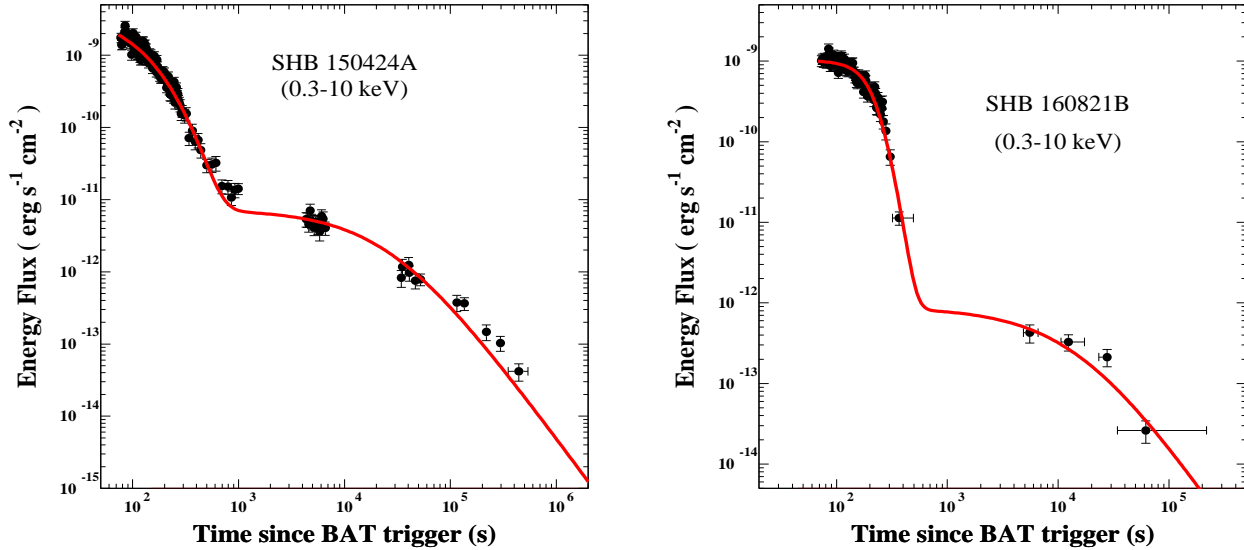


FIG. 9: The X-ray light curve of SHBs 150424A and 160821B reported in the Swift-XRT GRB light curve repository [16] and their best fit light curves assuming ICS of GC light by a highly relativistic jet taken over by MSP afterglow, as given by Eq.(4) or Eq.(10) with the 2 or 4 parameters, respectively, listed in Table I.

TABLE I: The best fit values of the parameters of Eq.(10) obtained from the 20 well-sampled X-ray afterglows of SHBs measured with the Swift-XRT [14] and shown in Figures. 6-9 [16]. Also listed are the values of the period and polar magnetic field of the MSPs at birth, as estimated from F_p and t_b for those SHBs with secured identity and redshift.

SHB	z	F_{ee} [$erg/s\ cm^2$]	a	t_{ee} [s]	F_p [$erg/s\ cm^2$]	t_b [s]	χ^2/dof	P [ms]
051210		1.04E-9	1.55	113			1.62	
051221A	0.5465	3.70E-8	[0]	570	2.59E-12	42522	1.44	3.53
051227	0.8	1.24E-9	1.33	103	6.88E-12	3829	0.95	1.39
060313		2.66E-10	1.4	199	2.54E-11	4932	0.89	
? 060614	0.125	1.64E-7	[0]	111	1.08E-11	49830	1.39	48.0
060801		1.32E-10	23.7	104			1.23	
061006		4.14E-9	[0]	1222	8.46E-13	33318	1.64	
? 070714B	0.92	1.8E-9	3.16	76	1.03E-10	736	1.41	6.50
070724A	0.457	2.11E-9	3.16	67	1.06E-12	19381	4.68	6.31
070809	0.2187	2.26E-11	1.18	183	3.14E-12	17512	1.22	7.82
071227	0.383	7.02E-10	80	51	3.86E-12	3079	1.97	3.98
080123	0.495 (?)	1.38E-9	199	43	8.20E-13	5536	1.93	
080503		7.74E-9	1.25	99			1.28	
090510	0.903				3.74E-10	546	1.83	7.04
120308A		9.94E-9	16	56	6.87E-11	4730	1.51	
130603B	0.3564				6.06E-11	3668	1.19	1.05
130912A		2.31E-10	[0]	1691	1.72E-12	17489	1.47	
150423A	1.394				1.26E-11	1312	1.35	0.60
150424A	1 ± .2	4.21E-9	[0]	140	7.25E-12	26524	1.53	1.08
160821B	0.16 (?)	1.03E-9	118	53	8.75E-13	15295	1.38	